Supplementary materials

Simultaneous Determination of Eight Cannabinoids in Hemp-Based Dietary Supplements via an Optimized SE-HPLC-PDA Workflow Integrating Chemometric Evaluation

Radosław Porada[1], Monika Wójcik[1], Małgorzata Herman[1*], Wojciech Piekoszewski[1]

[1] Department of Analytical Chemistry, Faculty of Chemistry, Jagiellonian University, Gronostajowa 2, 30-387 Kraków, Poland

[*]Corresponding author: malgorzata.herman@uj.edu.pl

Tab. S1. Comparison of chromatographic methods used to quantify a group of cannabinoids in samples of different matrix with the calculated LOD and LOQ values.

Analyte	**Samples**	**Method**	**Column**	**Extraction type/extraction solvent**	**LOD**	**LOQ**	**Ref.**
CBDA, CBD	Hemp oil	HPLC-PDA	Spheri-5, type C18 250 × 4.6 mm, 5 µm	Acetonitrile, Acetonitrile/Ethanol (v/v) 1:1, Ethanol	0.17-1.94 µg/mL	0.78-3.12 µg/mL	[5]
CBDA, CBD	Plant material	UHPLC-PDA	Fortis Speed Core C18-PFP 100 mm × 2.1 mm, 2.6 mm	UAE, DM, MAE, SFE	0.04-0.07 µg/mL	0.12-0.22 µg/mL	[6]
THCA, CBDA, Δ9-THC, CBD, CBC, CBN	Female inflorescences and cannabis resin	UHPLC-PDA	Phenomenex Luna Omega C18 150 × 2.1mm, 1.6 µm	Methanol	0.15-1.00 µg/mL	0.05-2.50 µg/mL	[7]
Δ^9-THC, CBD	Female inflorescences	HPLC-HRMS	Hypersil GOLD™ 100 × 2.1 mm, 1.9 µm	Methanol + ultrasonication	0.30-0.50 ng/mL	0.50 ng/mL	[8]
THCA, CBDA, Δ^9-THC, THCV, CBD, CBC, CBG, Δ^8-THC, CBN	Dried medical marijuana	HPLC-PDA	Kinetex®C18, 100 × 3.0 mm, 1.7 µm	Methanol/Chloroform (% v/v) 9:1	0.09 – 1.01 ppm	0.25-2.74 ppm	[9]
THCA, CBDA, Δ9-THC, CBD, CBN	Cannabis samples: flowers, mixed material consisting of leaves and stems without flowers, hashish	HPLC-PDA	Kinetex C8, 100 × 2.1 mm, 2.6 mm	Methanol/Hexane (% v/v) 9:1 + ultrasonication	0.30-0.50 µg/mL	1.00-10.00 µg/mL	[10]
CBGA, THCA, CBDA, Δ^9-THC, CBD, CBG, Δ^8-THC, CBN	Drug-type and nonpsychoactive cannabis	HPLC-PDA	Waters XTerra® MS C18, 250 × 2.1 mm, 5µm Waters XTerra® MS C18 guard column 10 × 2.1 mm, 5µm	Methanol/Chloroform (% v/v) 9:1	0.0625 – 0.25 µg/mL	0.125-0.375 µg/mL	[11]
CBDA, CBCA-A, Δ^9-THC, CBD, CBC, CBG, CBN	Tea and oil	UHPLC-MS/MS	Acquity UPLC HSS C18 150 × 2.1 mm, 1.8 µm	Methanol/Chloroform (% v/v) 9:1	0.30 µg/mL	1.00 µg/mL	[12]
THCA, Δ^9-THC, CBD,	Urine and oral fluid	GC-MS	Fused silica capillary column HP-5MS, 30 m, 0.25 mm i.d, film thickness 0.25 mm	Hexane/Ethyl acetate (% v/v) 9:1	0.20-0.30 ng/mL	0.80-0.90 ng/mL	[13]

CBGA, THCA, CBDA, Δ^9-THC, CBD, CBG, CBN	Female inflorescences	HPLC-PDA	Ascentis Express C18 150 × 3.0 mm, 2.7 µm	Ethanol	0.40-1.20 µg/mL	1.40-3.30 µg/mL	[14]
THCA, Δ^9-THC, CBD, CBN	Plant materials, food products	HPLC-PDA	ACE 5 C18-AR and the conventional C18 column	Ethanol	2.50 µg/g	10.00 µg/g	[15]
THCA, CBDA, Δ^9-THC, CBD, CBN	Hashish, marijuana, medical marijuana	HPLC-PDA-MS/MS	Waters Cortecs C18 100 × 2.1 mm, 2.7 µm	Acetonitrile, Methanol, Ethanol	0.03-0.50 ng/mL	0.10-0.20 ng/mL	[16]
CBDA, Δ^9-THC, CBD, CBN	Hemp oils	HPLC-PDA	Spheri-5, type C18 250 × 4.6 mm, 5 µm	Acetonitrile	0.17-1.94 µg/mL	0.78-5.03 µg/mL	[17]
CBGA, CBDA, CBD, CBG	Female inflorescences	HPLC-UV/PDA	Ascentis Express C18 150 × 3.0 mm, 2.7 µm	DM, UAE, MAE, SFE	0.50-0.80 µg/mL	1.08-2.50 µg/mL	[18]
CBGA, THCA-A, CBDA, Δ^9-THC, THCV, CBD, CBDV, CBC, CBG, Δ^8-THC, CBN	Cannabis based products: hemp seeds, cannabis enhanced beer, Energy drink, pralines, coffee, tea	HPLC-MS	Poroshell 120 EC-C18 50 × 4.6 mm, 2.7 µm	SPE, UAE, Soxhlet Extraction	0.94-2.19 ng/mL	2.83-6.95 ng/mL	[19]
CBGA, CBDA, CBG, CBD, THCV, CBN, 9-THC, THCA	Cannabis dietary supplement (oil/water-based, for humans and animals)	HPLC-PDA	C18 Brownlee columns 250 × 4.6 mm, 5 µm	LLE, Ethanol	2.1 µg/g	6.3 µg/g	This work

DM – Dynamic Maceration, UAE – Ultrasound Assisted Extraction, MAE – Microwaves Assisted Extraction, SFE – Supercritical Fluid Extraction, SPE – Solid Phase Extraction, HPLC-MS - High Performance Liquid Chromatography coupled to Mass Spectrometry, HRMS – High Resolution Mass Spectrometry, HPLC-PDA - High Performance Liquid Chromatography coupled to photodiode array detection, UHPLC – Ultrahigh Performance Liquid Chromatography, GC-MS – Gas Chromatography coupled to mass spectrometry

S1. HPLC-ESI-Q-TOF MS/MS analysis

Tab. S2. MS/MS detection and identification conditions of tested cannabinoids. *P* – precursor ion, R_1 - R_4 – reference ions.[1]

Analyte	Formula	Ionization mode	*P* (*m*/*z*)	R_1 (*m*/*z*)	R_2 (*m*/*z*)	R_3 (*m*/*z*)	R_4 (*m*/*z*)
THCV	$C_{19}H_{26}O_2$	ESI+	287.2006	165.0909	231.1381	203.1067	179.1067
CBD	$C_{21}H_{30}O_2$	ESI+	315.2319	193.1222	259.1694	233.1536	207.1380
Δ9-THC	$C_{21}H_{30}O_2$	ESI+	315.2319	193.1222	259.1694	233.1536	207.1380
CBG	$C_{21}H_{32}O_2$	ESI+	317.2475	193.1222	209.1070	123.0440	137.0598
CBN	$C_{21}H_{26}O_2$	ESI+	311.2006	223.1118	293.1900	241.1220	195.1169
THCA	$C_{22}H_{30}O_4$	ESI+	359.2217	341.2111	261.1485	233.1172	219.1016
CBDA	$C_{22}H_{30}O_4$	ESI+	359.2217	341.2111	261.1485	233.1172	219.1016
CBGA	$C_{22}H_{32}O_4$	ESI+	361.2373	343.2268	219.1016	177.0546	163.0390

S2. Optimization of separation and detection conditions

For the analysis of both acidic and neutral compounds in the reverse phase mode (C18 column), the pH of the mobile phase has to be lowered to shift the protonation-deprotonation equilibria towards uncharged forms. As such, these compounds are better retained at the chromatographic column, and the related peaks are symmetrical. Based on the literature study, a mobile phase composed of (A) H_2O + 0.5% (v:v) acetic acid and (B) ACN was chosen. The number of peaks (*N*), resolution (*R*), retention factors (*f*), and overall analysis time (t_a) were selected as the criteria during the optimization of conditions of chromatographic separation. As this poses a non-linear problem in multidimensional objective functions whose derivatives are unknown, considering that *N* can take only integer values, the Nelder-Mead simplex method (NMSM)[2] was selected. It involves a direct comparison of actual results to deduce the next conditions to be examined based on the predefined rules. The comparison can be either quantitative or qualitative, and the latter constitutes the advantage of NMSM over widely used factorial designs.[2]

In the first step, the time program of the gradient elution was optimized using the NMSM with the initial percentage of ACN and gradient slope as the independent variables. The latter was defined as the increase in ACN content over rise time, and at this stage, 10% increase in ACN content was assumed, and the flow rate was set to 1.0 mL min^{-1}, while the column oven was kept at 25 °C. At first, three starting points were selected (A, B, and C in Fig. S1A) and the corresponding chromatograms were recorded (Fig. S1B). They indicate that when the ACN content had been diminished, retention times of examined compounds and peak width increased, whereas their heights declined. In point A, eight peaks are visible with the second one being significantly higher than the others. It can result from the coelution of two compounds of comparable properties, and this assumption is confirmed by chromatograms recorded for points C and B in particular. Based on that, conditions corresponding to point B could be perceived as the best ones; however, under the predefined analysis time (20 min.), only seven compounds were eluted from the column. A similar division of the second peak was noted for point C with a shorter analysis time. Thus, considering the established criteria, C was chosen as the best, A as the second, and B as the worst.

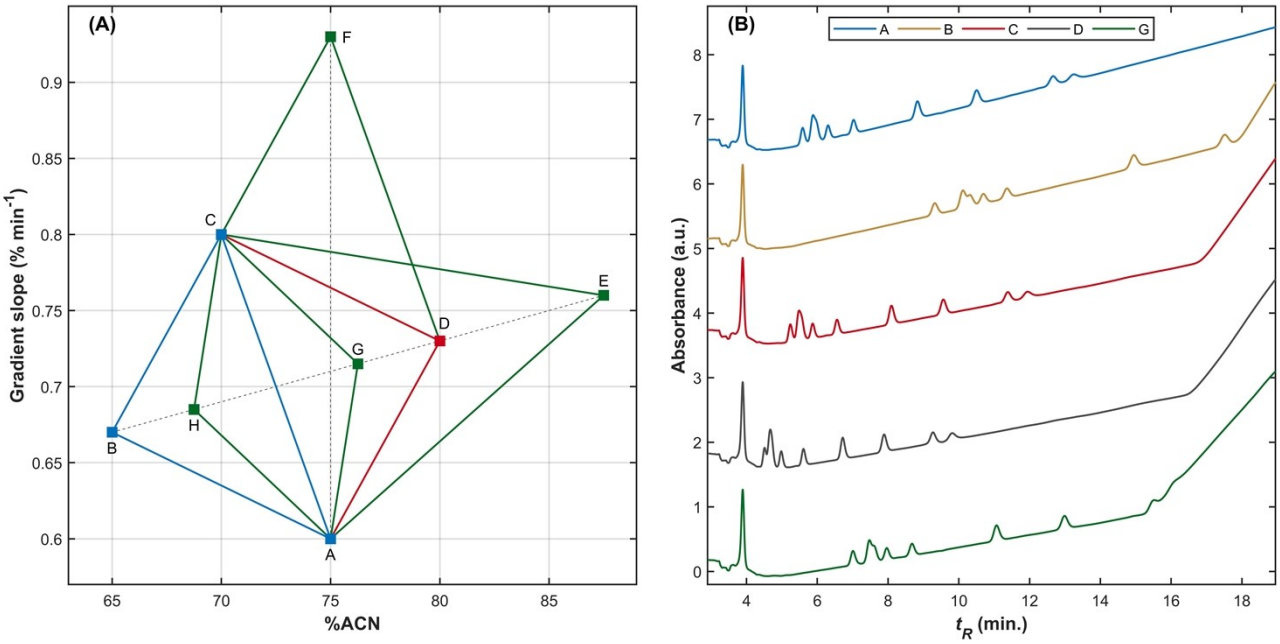

Fig. S1. (A) Optimization of the initial percentage of organic solvent (%ACN) and gradient slope via downhill simplex method. The starting conditions are marked in blue, red represents the product of symmetric reflection, whereas green illustrates four possible situations of further evolution. (B) Corresponding chromatograms recorded at λ = 220 nm with no baseline correction.

The next step in the NMSM is the symmetrical reflection of the worst point (here B) through the centroid of the remaining points, which in this case means the center of the AC line segment. The coordinates of the new point were calculated using the following formula:

$$x_D = (1 - Z) \cdot x_B + \frac{Z}{2} \cdot (x_A + x_C) \quad (1)$$

The value of Z depends on the performed operation and is equal to 2 for reflection. Thus, point D(80; 0.73) was obtained. Depending on the chromatogram recorded for this point, following situations are possible (marked in green in Fig. S1A):

1) D > C > A > B – if the best results were obtained for D, expansion of the worst point (point B) would be performed, and the coordinates of the new point E can be calculated using formula (1) setting Z = 3, thus E(87.5; 0.76).
2) C > D > A > B – if the new point was ordered as the second-best, the worst point would be discarded, and point A would be reflected through the centroid of the CD line segment, leading to point F(75.0; 0.93), whose coordinates can be calculated using formula (1) setting Z = 2.
3) C > A > D > B – if the response in point D was better only than the response in the worst point, simplex contraction would have been performed, and the coordinates of the new point would be calculated similarly to case 1) but with Z = 1.5, leading to G(76.25; 0.715).
4) C > A > B > D – if the response in point D was the worst among obtained so far, it would indicate that the optimal conditions are to be found inside the starting simplex ABC, hence, its contraction would be performed and the coordinates of the next point would be calculated using formula (1) setting Z = 0.5, leading to H(68.75; 0.685).

The next measurement was performed under conditions corresponding to point D. It resulted in the shortest analysis time, and the lowest separation between the first and the second peak (not a baseline

separation), caused by a too high amount of ACN at the beginning of its rapid increase. Nevertheless, an improvement in peak shape and overall analysis time is visible, hence, the response of point D was considered better than the response of B, but worse than that of A and C. Therefore, in the next step, simplex contraction was performed (case 3), and a chromatogram was recorded under the calculated conditions (point G). In it, nine peaks are visible, with the second and the third strongly overlapping each other. Additionally, the shape of the last two peaks exacerbated. To counteract these phenomena, the flow rate (v) of the mobile phase and the temperature of the column oven were varied. Lowering v to 0.6 mL min^{-1} increased the separation between the second and the third peak (some overlapping was still visible) and retention times of all tested compounds. Oven temperature, tested in the range from 15 to 40 °C with 5 °C increment, strongly influenced the separation of tested compounds. At 15 °C, only 7 peaks clearly were visible, and retention times were the highest. With every increase in the temperature, the separation and peak shape improved, and the time of analysis decreased. At 40°C, nine peaks can be clearly distinguished with the second and the third ones separated to the baseline. However, the separation of the first two peaks slightly diminished. Considering all that, flow rate of 0.6 mL min^{-1} and the temperature of 40 °C were selected for further optimization.

Based on the measurements conducted heretofore, several conclusions can be made. First, the temperature of 40 °C is crucial for the separation of the group of five peaks visible at low retention times. Moreover, higher %ACN in the mobile phase contributes to lower retention times and better peak shape (elevated peak height and lowered peak width), whereas low ACN content at the beginning is necessary to ensure the baseline separation of the five cannabinoids: CBDA, CBGA, CBG, CBD, and THCV. Thus, optimization of the initial %ACN and gradient slope *via* simplex method was repeated with the implementation of the inferred oven temperature (40 °C) and flow rate (0.6 mL min^{-1}). In contrast to the first attempt, studied parameters included the initial and maximum percentage of ACN. The starting points were located around the point G(76.25; 0.715), which previously gave the best results. The baseline separation of peaks corresponding to CBDA, CBGA, CBG, CBD, and THC, as well as between CBC and THCA, has been achieved for the gradient elution starting with 65% B, followed by a linear increase to 85% B at 15 min., return to 65% B at 25 min., and 2 min. of isocratic wash. These conditions were applied in the further measurements.

Several of the previously reported methods for cannabinoid determination used HPLC with UV detection employing a single wavelength, typically 220 nm.[3] However, as presented in Fig. S2, tested compounds contained within the mobile phase absorb light in the range from 200 to 330 nm with the highest absorption efficiency below 240 nm. It justifies the use of ACN instead of MeOH, as ACN has a shorter UV cutoff wavelength than MeOH has. Based on the recorded data, several wavelengths were selected for further consideration (Fig. S2B). The most apparent peaks were recorded at 220 nm, which is also reflected in the highest sensitivity of the calibration curves (see Section 3.2 and S4). Noticeable signals for all determined cannabinoids were obtained also at λ = 240 nm, but the intensities were significantly lower than for λ = 220 nm. However, for the latter, many small signals in the baseline were recorded, hindering peak analysis, whereas at 240 nm, the baseline exhibited little fluctuation. In the case of the acidic cannabinoids (CBDA, CBGA, THCA) and CBN, peaks at the wavelengths higher than 250 nm were manifested. Comparison of the UV spectrum and molecular structure of the acidic cannabinoids with their neutral counterparts (Fig. S2C and S2D) indicates that bands at 269 and 307 nm corresponds to the absorption by π-bonds in the carboxyl group. For

CBN, a wide band between 260 and 320 nm is visible. It results from the absorption of the moiety composed of the three fused rings: two benzene rings and one pyran rings. Their mutual arrangement enables the delocalization of π electrons over a higher number of carbon atoms, which explains the shift in absorption band towards higher wavelengths. Additionally, at wavelengths higher than 250 nm, the fluctuation of the baseline is extremely limited. Thus, the chromatograms recorded at λ = 307, 285, and 269 nm can be used to reliably determine acidic cannabinoids and CBN even in the presence of high concentrations of CBD and CBG.

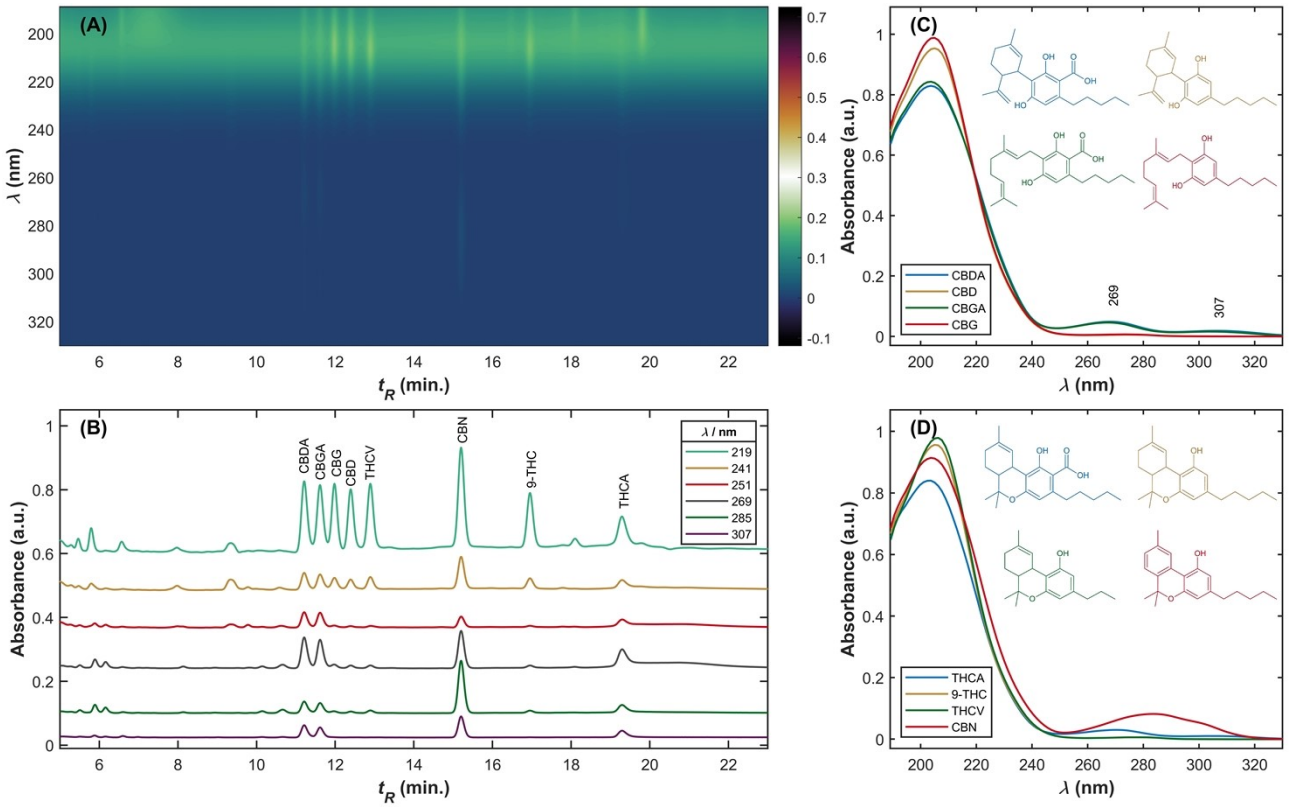

Fig. S2. Chromatograms (A) represented in the form of heat map and (B) for selected wavelengths. (C,D) UV spectra of analyzed cannabinoids with their structures.

S3. Optimization of extraction step

To find the best conditions of cannabinoids isolation from dietary supplements, studies on the spiked samples were performed. The following conditions were taken into consideration in the optimization: (a) type of extraction solvent (EtOH, MeOH); (b) volume of extraction solvent (1.0, 1.5, 2.0 mL); and (c) time of shaking the samples on a multi-functional rocker shaker (10, 15, 25 min.). Six samples weighing approximately 100 mg of olive oil were prepared for each set of extraction conditions and fortified with 5 µg of cannabinoid standards. Then, spiked samples were vortexed and incubated on a rocker shaker for 1 h at room temperature to ensure a homogenous distribution of cannabinoids in the matrix. Subsequently, such samples were subjected to the extraction procedure described in Section 2.4 with the adjustments needed to account for the tested variables. The peak area of each cannabinoid in the fortified olive oil after extraction (A_s) was compared to the peak area of each cannabinoid standard in MeOH (A_{st}) to calculate the extraction efficiency E_e:

$$E_e(\%) = (\mathrm{A_s}/\mathrm{A_{st}}) \cdot 100\%, \quad (2)$$

According to[4], it should be in the range of 80-120%.

Figure S3 presents the extraction efficiency values calculated for the successive stages of the optimization. Based on the performed experiments, following conclusions have been reached: (I) The usage of ethanol resulted in higher extraction efficiency for Δ9-THC, which is psychoactive and its content in products is regulated by law, as well as for CBN and THCA. For CBDA and CBD, the results obtained using both solvents were comparable (Fig. S3A); (II) the 1.5 mL volume of ethanol is more beneficial than the usage of 1 mL of solvent for all tested analytes. Although, using 2 mL of EtOH yielded higher extraction recovery for four compounds, the recovery was only slightly lower for Δ9-THC than in the case of using 1.5 mL EtOH (Fig. S3B); (III) a longer time of incubation on rocker shaker had a beneficial impact on generated extraction recovery values (Fig. S3C). Based on this, 25 minutes of incubation was chosen. The optimal conditions for extraction process were therefore 1.5 mL of ethanol and 25-minute incubation on rocker shaker. The small error bars indicate a particularly good repeatability of the extraction procedure.

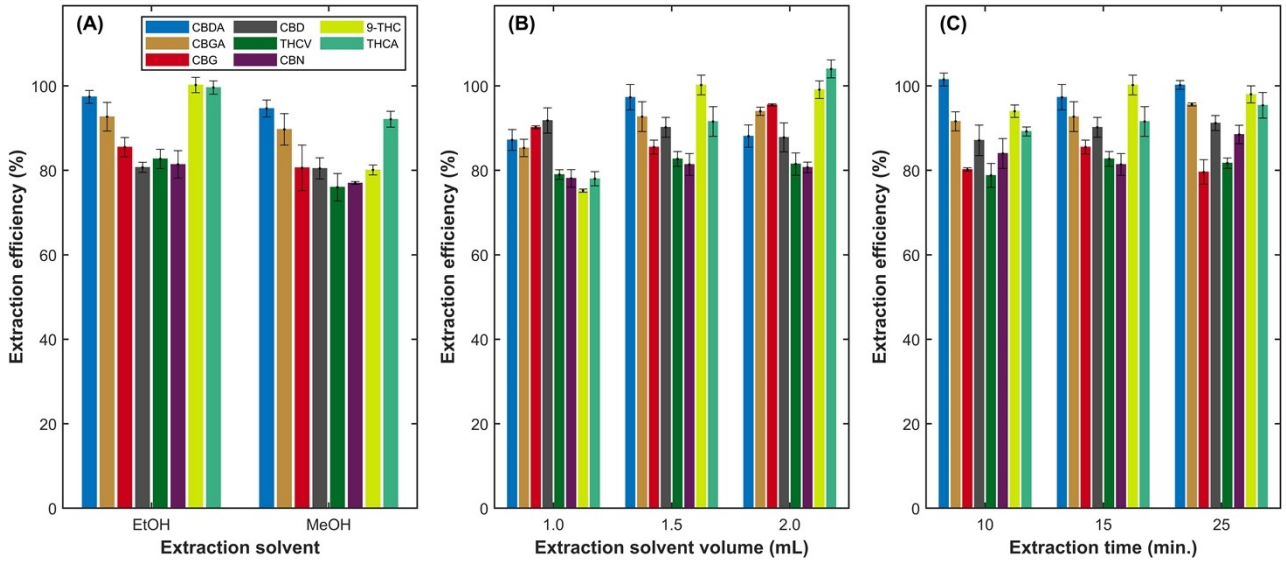

Fig. S3. Influence of (A) extraction solvent, (B) its volume, and (C) extraction time on the efficiency of cannabinoid extraction from oil matrix.

S4. Method validation

Tab. S3. Calibration curve parameters for detection wavelength of 220 nm. Linearity range of 0.625-10 (µg/100 mg) for each considered cannabinoid *)

Analyte	a (100 mg/µg)	S_a (100 mg/µg)	b	S_b
CBDA	48778.3	637.5	-6625.0	3003.6
CBGA	45684.4	382.2	1684.5	1801.0
CBG	43125.3	657.9	-5039.9	3100.0
CBD	39897.6	683.6	-6784.3	3220.8
THCV	42806.6	480.5	-1787.3	2264.1
CBN	67333.4	400.6	-4958.3	1887.4
9-THC	37304.9	309.3	-2939.1	1457.5
THCAA	28574.8	635.5	-6028.2	2994.2

*) fitting the linear function y=*a*x+*b*; *a* - slope of the straight line, *b* - intercept, S_a-standard deviation of *a* value, S_b-standard deviation of *b* value

Tab. S4. Comparison of the sensitivity of the method for determining the cannabinoid group depending on the wavelength used in the detector.

Analyte	Sensitivity $a \cdot 10^3$ (100 mg/µg)					
	220 (nm)	241 (nm)	251 (nm)	269 (nm)	285 (nm)	307 (nm)
CBDA	48.8 ± 0.8	13.7 ± 0.2	10.9 ± 0.2	21.1 ± 0.3	8.3 ± 0.1	8.4 ± 0.1
CBGA	45.7 ± 0.5	12.2 ± 0.2	10.6 ± 0.1	19.8 ± 0.3	7.3 ± 0.1	7.2 ± 0.1
CBG	43.1 ± 0.6	8.2 ± 0.1	1.18 ± 0.02	2.15 ± 0.04	0.93 ± 0.02	-
CBD	39.9 ± 0.3	7.53 ± 0.09	0.96 ± 0.02	1.98 ± 0.09	1.06 ± 0.02	-
THCV	42.8 ± 0.4	9.3 ± 0.1	1.09 ± 0.01	1.84 ± 0.02	1.77 ± 0.02	-
CBN	67.3 ± 0.7	23.8 ± 0.3	8.01 ± 0.08	25.9 ± 0.2	36.6 ± 0.3	15.8 ± 0.2
Δ^9-THC	37.3 ± 0.3	8.31 ± 0.07	1.01 ± 0.03	1.79 ± 0.02	1.48 ± 0.01	-
THCA-A	28.6 ± 0.4	9.4 ± 0.2	6.6 ± 0.1	16.7 ± 0.2	7.81 ± 0.07	7.43 ± 0.08

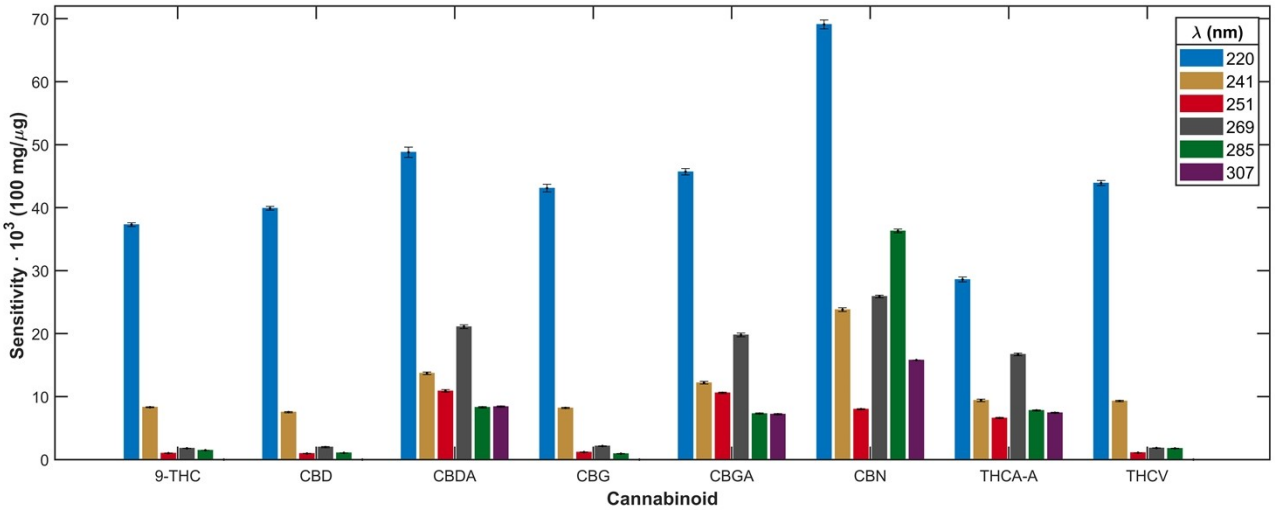

Fig. S4. Comparison of the sensitivity of cannabinoid determination depending on the detection wavelength.

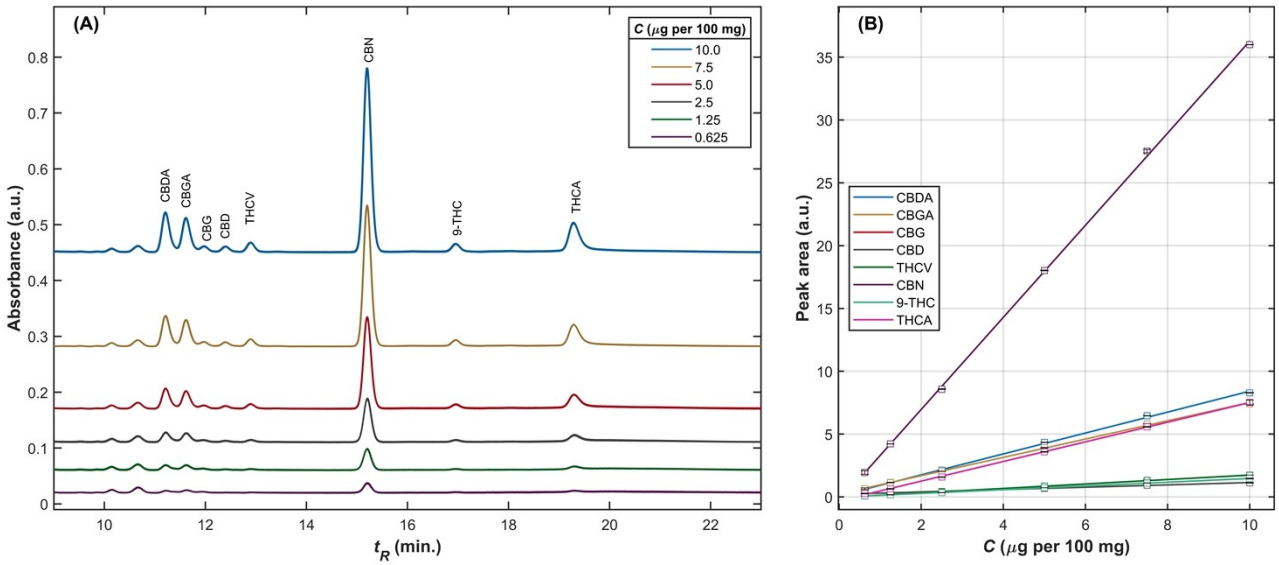

Fig. S5. (A) Chromatograms recorded at λ = 285 nm for the increasing concentrations of cannabinoids (three replicates for each concentration). (B) Corresponding calibration curves.

References

1 W. Kołodziej, M. Herman, W. Piekoszewski and R. Porada, *Microchemical Journal*, 2024, **203**, 110930.

2 M. H. Wright, *Documenta Mathematica*, 2012, 271–276.

3 B. Piani, C. Ferfuia, R. Bortolomeazzi, G. Verardo and M. Baldini, *Food Anal. Methods*, 2022, **15**, 1677–1686.

4 A. Nemeškalová, K. Hájková, L. Mikulů, D. Sýkora and M. Kuchař, *Talanta*, 2020, **219**, 121250.

5 K. Madej, G. Kózka, M. Winiarski and W. Piekoszewski, *Separations*, 2020, **7**, 1–10.

6 P. S. Tzimas, E. A. Petrakis, M. Halabalaki and L. A. Skaltsounis, *Anal. Chim. Acta*, 2021, **1150**, 338200.

7 A. C. Elkins, M. A. Deseo, S. Rochfort, V. Ezernieks and G. Spangenberg, *J. Chromatogr. B Analyt. Technol. Biomed. Life Sci.*, 2019, **1109**, 76–83.

8 M. C. Monti, P. Frei, S. Weber, E. Scheurer and K. Mercer-Chalmers-Bender, *Anal. Bioanal. Chem.*, 2022, **414**, 3847–3862.

9 E. M. Mudge, S. J. Murch and P. N. Brown, *Anal. Bioanal. Chem.*, 2017, **409**, 3153–3163.

10 M. Hädener, S. König and W. Weinmann, *Forensic Sci. Int.*, 2019, **299**, 142–150.

11 B. De Backer, B. Debrus, P. Lebrun, L. Theunis, N. Dubois, L. Decock, A. Verstraete, P. Hubert and C. Charlier, *Journal of Chromatography B*, 2009, **877**, 4115–4124.

12 R. Pacifici, E. Marchei, F. Salvatore, L. Guandalini, F. P. Busardò and S. Pichini, *Clin. Chem. Lab. Med.*, 2017, **55**, 1555–1563.

13 R. Pacifici, S. Pichini, M. Pellegrini, R. Tittarelli, F. Pantano, G. Mannocchi, M. C. Rotolo and F. P. Busardò, *Clin. Chem. Lab. Med.*, 2019, **57**, 238–243.

14 V. Brighenti, L. Marchetti, L. Anceschi, M. Protti, P. Verri, F. Pollastro, L. Mercolini, D. Bertelli, C. Zanardi and F. Pellati, *J. Pharm. Biomed. Anal.*, DOI:10.1016/j.jpba.2021.114346.

15 L. A. Ciolino, T. L. Ranieri and A. M. Taylor, *Forensic Sci. Int.*, 2018, **289**, 438–447.

16 M. Protti, V. Brighenti, M. R. Battaglia, L. Anceschi, F. Pellati and L. Mercolini, *ACS Med. Chem. Lett.*, 2019, **10**, 539–544.

17 K. Madej, A. Chmiołek, K. Szlachta and W. Piekoszewski, *Separations*, 2021, **8**, 227.

18 V. Brighenti, F. Pellati, M. Steinbach, D. Maran and S. Benvenuti, *J. Pharm. Biomed. Anal.*, 2017, **143**, 228–236.

19 M. C. Christodoulou, A. Christou, I. J. Stavrou and C. P. Kapnissi-Christodoulou, *Journal of Food Composition and Analysis*, 2023, **115**, 104915.